International Journal of Engineering Research and Advanced Technology (IJERAT)

E-ISSN : 2454-6135

DOI: http://dx.doi.org/10.7324/IJERAT.2018.3188

Volume.4, Issue 2

February-2018

Validation of Finite Element Method in the Analysis of Biaxial Buckling of Thin Laminated Plates

Osama Mohammed Elmardi Suleiman[1], Mahmoud Yassin Osman[2] and Tagelsir Hassan[3]

Assistant Professor[1], Professor[2] and Associate Professor[3]

[1]Department of Mechanical Engineering,

Faculty of Engineering and Technology, Nile Valley University, Atbara,

River Nile State,

[2]Department of Mechanical Engineering,

Kassala University, Kassala,

[3]Department of Mechanical Engineering,

Omdurman Islamic University, Omdurman,

Sudan

ABSTRACT

Finite element (FE) method is presented for the analysis of thin rectangular laminated composite plates under the biaxial action of in – plane compressive loading. The analysis uses the classical laminated plate theory (CLPT) which does not account for shear deformations. In this theory it is assumed that the laminate is in a state of plane stress, the individual lamina is linearly elastic, and there is perfect bonding between layers. The classical laminated plate theory (CLPT), which is an extension of the classical plate theory (CPT) assumes that normal to the mid – surface before deformation remains straight and normal to the mid – surface after deformation. Therefore, this theory is only adequate for buckling analysis of thin laminates. A Fortran program has been compiled. The convergence and accuracy of the FE solutions for biaxial buckling of thin laminated rectangular plates are established by comparison with various theoretical and experimental solutions. The good agreement of comparisons demonstrates the reliability of finite element methods used.

Keywords: *Validation of finite element method, Classical laminated plate theory, Buckling, Thin plates, Laminated Composites.*

1. INTRODUCTION

From the point of view of solid mechanics, the deformation of a plate subjected to transverse and / or in plane loading consists of two components: flexural deformation due to rotation of cross – sections, and shear deformation due to sliding of section or layers. The resulting deformation depends on two parameters: the thickness to length ratio and the ratio of elastic to shear moduli. When the thickness to length ratio is small, the plate is considered thin, and it deforms mainly by flexure or bending; whereas when the thickness to length and the modular ratios are both large, the plate deforms mainly through shear. Due to the high ratio of in – plane modulus to transverse shear modulus, the shear deformation effects are more pronounced in the composite laminates subjected to transverse and / or in – plane loads than in the isotropic plates under similar loading conditions.

In the present work, the analysis uses the classical laminated plate theory (CLPT) which does not account for transverse shear deformations. This theory is applicable to homogeneous thin plates (i.e. the length to thickness ratio $a/h > 20$). The classical laminated plate theory (CLPT), which is an extension of the classical plate theory (CPT) applied to laminated plates was the first theory formulated for the analysis of laminated plates by Reissner and Stavsky [1] in 1961, in which the Kirchhoff and

Love assumption that normal to the mid – surface before deformation remain straight and normal to the mid – surface after deformation is used, but it is not adequate for the flexural analysis of moderately thick laminates. However, it gives reasonably accurate results for many engineering problems i.e. thin composite plates, as stated by Srinivas and Rao [2], Reissner and Stavsky [1].

The finite element method is formulated by the energy method. The numerical method can be summarized in the following procedures:

1. The choice of the element and its shape functions.
2. Formulation of finite element model by the energy approach to develop both element stiffness and differential matrices.
3. Employment of the principles of non – dimensionality to convert the element matrices to their non – dimensional forms.
4. Assembly of both element stiffness and differential matrices to obtain the corresponding global matrices.
5. Introduction of boundary conditions as required for the plate edges.
6. Suitable software can be used to solve the problem (here two software were utilized, FORTRAN and ANSYS).

2. MATHEMATICAL FORMULATION

Consider a thin plate of length a, breadth b, and thickness h as shown in Figure 2.1a, subjected to in – plane loads R_x , R_y and R_{xy} as shown in Figure 2.1b. The in – plane displacements $u(x,y,z)$ and $v(x,y,z)$, can be expressed in terms of the out – of – plane displacement $w(x,y)$ as shown below.

$$u = -z\frac{\partial w}{\partial x} \qquad (1)$$

$$v = -z\frac{\partial w}{\partial y}$$

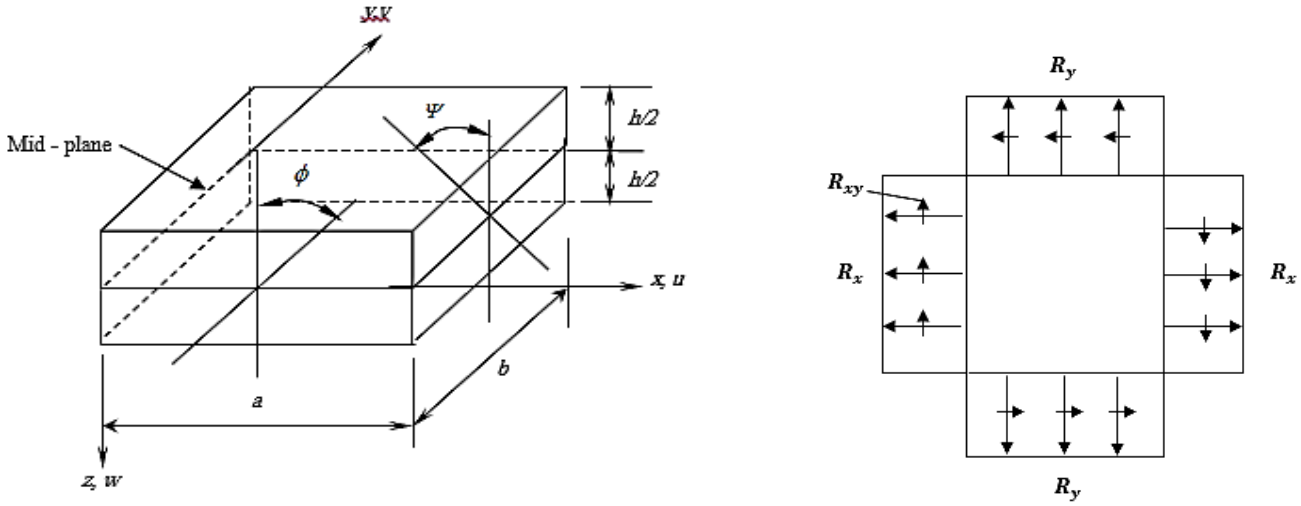

(a) **(b)**

Figure 2.1

The strain – displacement relations according to the large deformation theory are:

$$\epsilon_x = \frac{\partial u}{\partial x} + \frac{1}{2}\left(\frac{\partial w}{\partial x}\right)^2 = -z\frac{\partial^2 w}{\partial x^2} + \frac{1}{2}\left(\frac{\partial w}{\partial x}\right)^2$$

$$\epsilon_y = \frac{\partial v}{\partial y} + \frac{1}{2}\left(\frac{\partial w}{\partial y}\right)^2 = -z\frac{\partial^2 w}{\partial y^2} + \frac{1}{2}\left(\frac{\partial w}{\partial y}\right)^2$$

$$\epsilon_{xy} = \frac{\partial v}{\partial x} + \frac{\partial u}{\partial y} + \frac{\partial w}{\partial x}\frac{\partial w}{\partial y} = -2z\frac{\partial^2 w}{\partial x\,\partial y} + \frac{\partial w}{\partial x}\frac{\partial w}{\partial y}$$

These can be written as:

$$\epsilon = \epsilon_1 + \epsilon_2$$

Where, $\epsilon = [\epsilon_x\ \epsilon_y\ \epsilon_{xy}]^T$ and ϵ_1 and ϵ_2 represent the linear and non – linear parts of the strain, i.e.

$$\epsilon_1 = -z\left[\frac{\partial^2 w}{\partial x^2} \quad \frac{\partial^2 w}{\partial y^2} \quad 2\frac{\partial w}{\partial x\,\partial y}\right]^T \qquad (2)$$

$$\epsilon_2 = \frac{1}{2}\left[\left(\frac{\partial w}{\partial x}\right)^2 \quad \left(\frac{\partial w}{\partial y}\right)^2 \quad 2\frac{\partial w}{\partial x}\frac{\partial w}{\partial y}\right]^T \qquad (3)$$

The virtual linear strains can be written as:

$$\delta\,\epsilon_1 = -z\left[\frac{\partial^2}{\partial x^2} \quad \frac{\partial^2}{\partial y^2} \quad 2\frac{\partial^2}{\partial x\,\partial y}\right]^T \delta\, w \qquad (4)$$

The virtual linear strains energy

$$\delta\, U = \int_V \delta\epsilon_i^T \sigma\, dV \qquad (5)$$

Where V denotes volume

The stress – strain relations,

$$\sigma = C\,\epsilon_1$$

Where C are the material properties given in Appendix (A).

Substitute the above equation in equation (5).

$$\delta\, U = \int_V \delta\epsilon_1^T C\,\epsilon_1^T dV \qquad (6)$$

Now express w in terms of the shape functions N (given in Appendix (B)) and nodal displacements a^e , equation (2) can be written as:

$$\delta\,\epsilon_1 = -Z\,B\,\delta\,a^e$$

Where,

$$B_i = \left[\frac{\partial^2 N_i}{\partial x^2} \quad \frac{\partial^2 N_i}{\partial y^2} \quad 2\frac{\partial^2 N_i}{\partial x\,\partial y}\right]^T$$

Hence equation (6) can be written in the form,

$$\delta\, U = \int_V (B\,\delta\,a^e)^T (C\,z^2)\,(B\,a^e)\,dV$$

or

$$\delta\, U = \delta\, a^{eT} \int B^T D\, B\, a^e\, dx\, dy$$

Where,

$$D = \sum_{k=1}^{n} \int_{z_{k-1}}^{z_k} C\, z^2\, dz$$

Hence, the virtual strain energy,

$$\delta\, U = \delta\, a^{eT} K^e\, a^e \qquad (7)$$

Where K^e is the element stiffness matrix,

$$i.e. \qquad K^e = \int B^T D\, B\, dx\, dy \qquad (8)$$

Now equation (3) can be written in the form,

$$\epsilon_2 = \frac{1}{2}\begin{bmatrix} \frac{\partial w}{\partial x} & 0 \\ 0 & \frac{\partial w}{\partial y} \\ \frac{\partial w}{\partial y} & \frac{\partial w}{\partial x} \end{bmatrix}\begin{bmatrix} \frac{\partial w}{\partial x} \\ \frac{\partial w}{\partial y} \end{bmatrix}$$

The virtual strain,

$$\delta\,\epsilon_2 = \begin{bmatrix} \frac{\partial}{\partial x}\delta w & 0 \\ 0 & \frac{\partial}{\partial y}\delta w \\ \frac{\partial}{\partial y}\delta w & \frac{\partial}{\partial x}\delta w \end{bmatrix}\begin{bmatrix} \frac{\partial w}{\partial x} \\ \frac{\partial w}{\partial y} \end{bmatrix}$$

The virtual work,

$$\delta W = \int_V \delta \epsilon_i^T \sigma \, dV = \int_V \begin{bmatrix} \frac{\partial w}{\partial x} & \frac{\partial w}{\partial y} \end{bmatrix} \begin{bmatrix} \frac{\partial}{\partial x}\delta w & 0 & \frac{\partial}{\partial y}\delta w \\ 0 & \frac{\partial}{\partial y}\delta w & \frac{\partial}{\partial x}\delta w \end{bmatrix} \begin{bmatrix} \sigma_x \\ \sigma_y \\ \sigma_{xy} \end{bmatrix} dV$$

$$\delta W = \int \begin{bmatrix} \frac{\partial w}{\partial x} & \frac{\partial w}{\partial y} \end{bmatrix} \begin{bmatrix} \frac{\partial}{\partial x}\delta w & 0 & \frac{\partial}{\partial y}\delta w \\ 0 & \frac{\partial}{\partial y}\delta w & \frac{\partial}{\partial x}\delta w \end{bmatrix} \begin{bmatrix} R_x \\ R_y \\ R_{xy} \end{bmatrix} dx \, dy$$

Where,

$$[R_x, R_y, R_{xy}] = \int_{-h/2}^{h/2} [\sigma_x, \sigma_y, \sigma_{xy}] \, dz$$

And σ_x , σ_y , and σ_{xy} are the in – plane stresses.

The previous equation can be written as:

$$\delta W = \int \begin{bmatrix} \frac{\partial}{\partial x}\delta w & \frac{\partial}{\partial y}\delta w \end{bmatrix} \begin{bmatrix} R_x & R_{xy} \\ R_{xy} & R_y \end{bmatrix} \begin{bmatrix} \frac{\partial w}{\partial x} \\ \frac{\partial w}{\partial y} \end{bmatrix} dx \, dy$$

Introducing the shape functions and nodal displacements, we get:

$$\delta W = \delta a^{e\,T} \int \begin{bmatrix} \frac{\partial N_i}{\partial x} & \frac{\partial N_i}{\partial y} \end{bmatrix} \begin{bmatrix} R_x & R_{xy} \\ R_{xy} & R_y \end{bmatrix} \begin{bmatrix} \frac{\partial N_j}{\partial x} \\ \frac{\partial N_j}{\partial y} \end{bmatrix} a^e \, dx \, dy$$

Now, let $R_x = -P_x,\ R_y = -P_y, and\ R_{xy} = -P_{xy}$

$$\delta W = -\delta a^{e^T} P_x K^{eD} a^e \qquad (9)$$

Where,

$$K^{eD} = \int \begin{bmatrix} \frac{\partial N_i}{\partial x} & \frac{\partial N_i}{\partial y} \end{bmatrix} \begin{bmatrix} 1 & \frac{P_{xy}}{P_x} \\ \frac{P_{xy}}{P_x} & \frac{P_y}{P_x} \end{bmatrix} \begin{bmatrix} \frac{\partial N_j}{\partial x} \\ \frac{\partial N_j}{\partial y} \end{bmatrix} dx \, dy \qquad (10)$$

K^{eD} is the element differential matrix.

Now,

$$\delta U + \delta W - 0$$

i.e.

$$\delta a^{e^T} K^e a^e - \delta a^{e^T} P_x K^{eD} a^e = 0$$

Now since δa^{e^T} is arbitrary and cannot be equal to zero, it follows that,

$$[K^e - P_x K^{eD}] a^e = 0$$

When the plate is divided into a number of elements, the global equation is:

$$[K - P_x K^D] a = 0 \qquad (11)$$

Where,

$$K = \sum K^e, \quad K^D = \sum K^{eD}, a = \sum a^e$$

Since, $a \neq 0$, then the determinant,

$$|K - P_x K^D| = 0 \qquad (12)$$

Hence, the buckling loads P_x and the buckling modes can be evaluated.

The elements of the stiffness matrix are obtained from equation (8) which can be expanded as follows:

$$K_{ij}^e = \int \begin{bmatrix} \frac{\partial^2 N_i}{\partial x^2} & \frac{\partial^2 N_i}{\partial y^2} & 2\frac{\partial^2 N_i}{\partial x \, \partial y} \end{bmatrix} \begin{bmatrix} D_{11} & D_{12} & D_{16} \\ D_{12} & D_{22} & D_{26} \\ D_{16} & D_{26} & D_{66} \end{bmatrix} \begin{bmatrix} \frac{\partial^2 N_j}{\partial x^2} \\ \frac{\partial^2 N_j}{\partial y^2} \\ 2\frac{\partial^2 N_j}{\partial x \partial y} \end{bmatrix} dx \, dy$$

i.e.

$$K_{ij}^e = \int \left[D_{11} \frac{\partial^2 N_i}{\partial x^2} \frac{\partial^2 N_j}{\partial x^2} + D_{12} \left(\frac{\partial^2 N_i}{\partial y^2} \frac{\partial^2 N_j}{\partial x^2} + \frac{\partial^2 N_i}{\partial x^2} \frac{\partial^2 N_j}{\partial y^2} \right) \right.$$
$$\left. + D_{22} \frac{\partial^2 N_i}{\partial y^2} \frac{\partial^2 N_j}{\partial y^2} + 4D_{66} \frac{\partial^2 N_i}{\partial x \, \partial y} \frac{\partial^2 N_i}{\partial x \, \partial y} + 2D_{16} \left(\frac{\partial^2 N_i}{\partial x \, \partial y} \frac{\partial^2 N_j}{\partial x^2} + \frac{\partial^2 N_i}{\partial x^2} \frac{\partial^2 N_j}{\partial x \, \partial y} \right) \right.$$

$$+2D_{26}\left(\frac{\partial^2 N_i}{\partial x\,\partial y}\frac{\partial^2 N_j}{\partial y^2}+\frac{\partial^2 N_i}{\partial y^2}\frac{\partial^2 N_j}{\partial x\,\partial y}\right)\Bigg]dxdy \quad (13)$$

The elements of the differential matrix are obtained from equation (10) which when expanded becomes:

$$K_{ij}^{eD}=\int\left[\frac{\partial N_i}{\partial x}\frac{\partial N_j}{\partial x}+\frac{P_{xy}}{P_x}\left(\frac{\partial N_i}{\partial y}\frac{\partial N_j}{\partial x}+\frac{\partial N_i}{\partial x}\frac{\partial N_j}{\partial y}\right)+\frac{P_y}{P_x}\frac{\partial N_i}{\partial y}\frac{\partial N_j}{\partial y}\right]dx\,dy \quad (14)$$

The integrals in equations (13) and (14) are given in Appendix (C). We use a 4 – noded element as shown in Figure 2.2 below.

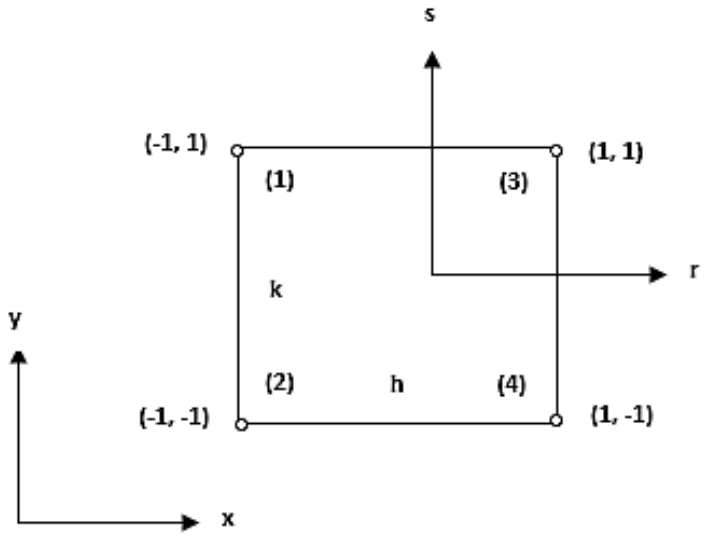

Figure 2.2

From the shape functions for the 4 – noded element expressed in global coordinates(x, y). We take:

$$w = N_1w_1 + N_2\phi_1 + N_3\psi_1 + N_4w_2 + N_5\phi_2 + N_6\psi_2$$
$$+N_7w_3 + N_8\phi_3 + N_9\psi_3 + N_{10}w_4 + N_{11}\phi_4 + N_{12}\psi_4$$

$$\text{where,} \qquad \phi = \frac{\partial w}{\partial x}, \qquad \text{and} \quad \psi = \frac{\partial w}{\partial y}$$

The shape functions in local coordinates (r, s) are as follows:

$$N_i = a_{i,1} + a_{i,2}r + a_{i,3}s + a_{i,4}r^2 + a_{i,5}rs + a_{i,6}s^2 + a_{i,7}r^3$$
$$+a_{i,8}r^2s + a_{i,9}rs^2 + a_{i,10}s^3 + a_{i,11}r^3s + a_{i,12}rs^3$$

Where , $i = 1, 2, 3, \ldots, 12$

The coefficients $a_{i,1}, a_{i,2}, etc$ are given in Appendix (B).

In the analysis, the following nondimensional quantities are used:

$$\bar{w} = \left(\frac{1}{h}\right)w\ , \qquad \bar{\phi} = \left(\frac{h}{a}\right)\phi\ , \quad \bar{\psi} = \left(\frac{h}{a}\right)\psi$$

$$\bar{D} = \left(\frac{1}{E\,h^3}\right)D\ , \qquad \bar{P} = \left(\frac{a^2}{E\,h^3}\right)P\ , \quad \bar{b} = b/a$$

3. BOUNDARY CONDITIONS

All of the analyses described in the present paper have been undertaken assuming the plate to be subjected to identical and/ or different support conditions on the four edges of the plate. The three sets of the of the edge conditions used here are designated as clamped – clamped (CC), simply – simply supported (SS), clamped – simply supported (CS), are shown in table 3.1 below.

Table 3.1 Boundary conditions

Boundary Conditions	**Plate dimensions in y – coordinate** $x = 0, x = a$	**Plate dimensions in x – coordinate** $y = 0, y = b$
CC	$w = \phi = \psi = 0$	$w = \phi = \psi = 0$
SS	$w = \psi = 0$	$w = \phi = 0$
CS	$w = \phi = \psi = 0$	$w = \phi = 0$

4. VALIDATION OF THE FINITE ELEMENT (FE) PROGRAM

In order to check the validity, applicability and accuracy of the present FE method, many comparisons were performed. The comparisons include theoretical, ANSYS simulation and experimental results.

4.1 Comparisons with Theoretical Results

In table 4.2 the non – dimensional critical buckling load is presented in order to compare with References [3], [4] and [5] for an isotropic plate of material 1 with different aspect ratios. As the table shows, the present results have a good agreement with References [3], [4] and [5].

Table 4.2 Comparison of the non – dimensional critical buckling load $\bar{P} = Pa^2/D$ for an isotropic plate (material 1)

Aspect Ratio a/b	References			
	Ref. [3]	Ref. [4]	Ref. [5]	Present Study
0.5	12.33	12.3370	12.3370	12.3
1.0	19.74	19.7392	19.7392	19.7

Table 4.3 below shows the effect of plate aspect ratio and modulus ratio on non – dimensional critical loads $\bar{P} = P(b^2\pi^2/D_{22})$ of rectangular laminates under biaxial compression. The following material properties were used: material 2: $E_1/E_2 = 5,\ 10,\ 20, 25$ and 40; $G_{12} = G_{13} = G_{23} = 0.5\ E_2$; $\nu_{12} = 0.25$ and $a/h = 20$. It is observed that the non – dimensional buckling load increases for symmetric laminates as the modular ratio increases. The present results were compared with Osman [6] and Reddy [7]. The verification process showed good agreement especially as the aspect ratio increases and the modulus ratio decreases.

Table 4.3 Buckling load for (0/ 90/ 90/ 0) simply supported (SS) plate for different aspect and moduli ratios under biaxial compression (material 2)

Aspect Ratio a/b	Modular Ratio	Biaxial Compression				
	E_1/E_2	5	10	20	25	40
0.5	Present	10.864	12.122	13.215	13.726	14.000
	Ref. [6]	-	12.307	-	13.689	-
	Ref. [7]	11.120	12.694	13.922	14.248	14.766
1.0	Present	2.790	3.130	3.430	3.510	3.645
	Ref. [6]	-	3.137	-	3.502	-
	Ref. [7]	2.825	3.174	3.481	3.562	3.702
1.5	Present	1.591	1.602	1.611	1.613	1.617
	Ref. [6]	-	1.605	-	1.606	-
	Ref. [7]	1.610	1.624	1.634	1.636	1.641

Table 4.4 shows the effect of plate aspect ratio, and modulus ratio on non – dimensional critical buckling loads $\bar{P} = P(b^2/\pi^2 D_{22})$ of simply supported (SS) antisymmetric cross – ply rectangular laminates under biaxial compression. The properties of material 2 were used. It is observed that the non – dimensional buckling load decreases for antisymmetric laminates as the modulus ratio increases. The present results were compared with Reddy [7]. The validation process showed good agreement especially as the aspect ratio increases and the modulus ratio decreases.

Table 4.4 Buckling load for (0/ 90/ 90/ 0) simply supported (SS) plate for different aspect and moduli ratios under biaxial compression (material 2)

Aspect Ratio a/b	Modular Ratio	Biaxial Compression				
	E_1/E_2	5	10	20	25	40
0.5	Present	4.000	3.706	3.535	3.498	3.442
	Ref. [7]	3.764	3.325	3.062	3.005	2.917
1.0	Present	1.395	1.209	1.102	1.079	1.045
	Ref. [7]	1.322	1.095	0.962	0.933	0.889
1.5	Present	1.069	0.954	0.889	0.875	0.853
	Ref. [7]	1.000	0.860	0.773	0.754	0.725

Table 4.5 below shows the effect of plate aspect ratio, and modulus ratio on non – dimensional critical buckling loads of simply supported (SS) antisymmetric angle – ply rectangular laminates under biaxial compression. The properties of material 2 were used. It is observed from table 4.5 that the prediction of the buckling loads by the present study is closer to that of Osman [6] and Reddy [7].

Table 4.5 Buckling load for antisymmetric angle – ply $(45/-45)_4$ plate with different moduli and aspect ratios under biaxial compression (material 2)

Aspect Ratio a/b	Modular Ratio	Biaxial Compression			
	E_1/E_2	10	20	25	40
0.5	Present	19.376	36.056	44.400	69.440
	Ref. [6]	19.480	-	44.630	-
	Ref. [7]	18.999	35.076	43.110	67.222
1.0	Present	9.028	17.186	21.265	33.512
	Ref. [6]	9.062	-	21.345	-
	Ref. [7]	8.813	16.660	20.578	32.343
1.5	Present	6.144	11.596	14.322	22.013
	Ref. [6]	6.170	-	14.383	-
	Ref. [7]	6.001	11.251	13.877	21.743

In tables 4.6 and 4.7, the buckling loads for symmetrically laminated composite plates of layer orientation (0/ 90/ 90/ 0) have been determined for three different aspect ratios ranging from 0.5 to 1.5 and two modulus ratios 40 and 5 of material 2. It is observed that the buckling load increases with increasing aspect ratio for biaxial compression loading. The buckling load is maximum for clamped – clamped (CC), and clamped – simply supported (CS) boundary conditions, while minimum for simply – simply supported (SS) boundary conditions. It is seen from tables 4.6 and 4.7 that the values of buckling loads by the present study is much closer to the of Osman [6].

Table 4.6 Buckling load for (0/ 90/ 90/ 0) plate with different boundary conditions and aspect ratios under biaxial compression $(\bar{P} = Pa^2/E_1h^3)$ (material 2) $E_1/E_2 = 40$; $G_{12} = G_{13} = G_{23} = 0.5\,E_2$; and $\nu_{12} = 0.25$

Aspect Ratio a/b	Comparisons of Results	Boundary Conditions		
		CC	SS	CS
0.5	Present	1.0742	0.4143	0.9679
	Ref. [6]	1.0827	0.4213	1.0022
1.0	Present	1.3795	0.4409	1.0723
	Ref. [6]	1.3795	0.4411	1.0741
1.5	Present	1.6402	0.4400	1.2543
	Ref. [6]	1.6367	0.4391	1.2466

Table 4.7 Buckling load for (0/ 90/ 90/ 0) plate with different boundary conditions and aspect ratios $(\bar{P} = Pa^2/E_1h^3)$ (material 2) $E_1/E_2 = 5$; $G_{12} = G_{13} = G_{23} = 0.5\,E_2$; and $\nu_{12} = 0.25$

Aspect Ratio a/b	Comparisons of Results	Boundary Conditions		
		CC	SS	CS
0.5	Present	1.7786	0.6787	1.6325
	Ref. [6]	1.8172	0.6877	1.6838
1.0	Present	2.1994	0.6972	1.8225
	Ref. [6]	2.2064	0.6985	1.8328
1.5	Present	2.7961	0.8943	1.7643
	Ref. [6]	2.8059	0.8962	1.7618

The same behavior of buckling load applies to symmetrically laminated composite plates (0/ 90/ 0) as shown in tables 4.8 and 4.9.

Table 4.8 Buckling load for (0/ 90/ 0) plate with different boundary conditions and aspect ratios ($\bar{P} = Pa^2/E_1h^3$) (material 2) $E_1/E_2 = 40$; $G_{12} = G_{13} = G_{23} = 0.5\,E_2$; and $\nu_{12} = 0.25$

Aspect Ratio a/b	Comparisons of Results	Boundary Conditions		
		CC	SS	CS
0.5	Present	1.7471	0.3238	0.6870
	Ref. [6]	0.7529	0.3325	0.7201
1.0	Present	0.9523	0.3485	0.7925
	Ref. [6]	0.9511	0.3489	0.7932
1.5	Present	1.1811	0.3530	0.8190
	Ref. [6]	1.1763	0.3514	0.8099

Table 4.9 Buckling load for (0/ 90/ 0) plate with different boundary conditions and aspect ratios ($\bar{P} = Pa^2/E_1h^3$) (material 2) $E_1/E_2 = 5$; $G_{12} = G_{13} = G_{23} = 0.5\,E_2$; and $\nu_{12} = 0.25$

Aspect Ratio a/b	Comparisons of Results	Boundary Conditions		
		CC	SS	CS
0.5	Present	1.6947	0.6772	1.5842
	Ref. [6]	1.7380	0.6871	1.6337
1.0	Present	2.1669	0.6970	1.7009
	Ref. [6]	2.1744	0.6984	1.7113
1.5	Present	2.5008	0.8224	1.7658
	Ref. [6]	2.5075	0.8235	1.7622

4.2.2 Comparisons with the Results of ANSYS Package

ANSYS is a general-purpose finite element modeling package for numerically solving a wide variety of mechanical problems. These problems include: static/ dynamic structural analysis (both linear and non – linear), heat transfer and fluid problems, as well as acoustic and electromagnetic problems. The problem of buckling in ANSYS is considered as static analysis.

To validate the present results with ANSYS, the present results were converted from its non – dimensional form to the dimensional form by using the formula $\bar{P} = Pa^2/E_1h^3$. The E – glass/ Epoxy material is selected to obtain the numerical results for the comparisons. The mechanical properties of this material (material 3) is given in table 4.10 below.

Table 4.10 Mechanical Properties of the E – glass/ Epoxy material (material 3)

Property	Value
E_1 or E_x	38.6 GN/m^2
E_2 or E_y	8.27 GN/m^2
G_{12} or G_{xy}	4.14 GN/m^2
G_{13} or G_{xz}	4.14 GN/m^2
G_{23} or G_{yz}	3.4 GN/m^2
ν_{12} or ν_{xy}	0.28

Tables 4.11 to 4.14 shows comparisons between the results of the present study and that simulated by ANSYS technique. Table 4.11 shows the effect of boundary conditions on dimensional buckling loads of symmetric angle – ply (30/ -30/ -30/ 30) of square thin laminates ($a/h = 20$) under biaxial compression. The properties of material 3 in table (4.10) were used. Small differences were shown between the results of the two techniques. The difference ranges between 0.6% to less than 2%. It is observed that as the mode serial number increases, the difference increases. The same behavior of buckling load of both techniques applies to symmetrically laminated composite plates of the order (45/ -45/ -45/ 45), (60/ -60/ -60/ 60) and (0/ 90/ 90/ 0) shown in tables (4.12), (4.13) and (4.14).

Table 4.11 Dimensional buckling load of symmetric angle–ply (30/ -30/ -30/ 30) square thin laminates with different boundary conditions (a/h=20) (material 3)

Boundary Conditions	Method	Mode Serial Number		
		1	2	3
SS	Present	109.5 N	193.4 N	322.8 N
	ANSYS	109.4 N	206.5 N	315.8 N
CS	Present	234.7 N	257.2 N	371.41 N
	ANSYS	233.21 N	255.6 N	378.7 N

Table 4.12 Dimensional buckling load of symmetric angle–ply (45/-45/-45/45) square thin laminates with different boundary conditions (a/h=20) (material 3)

Boundary Conditions	Method	Mode Serial Number		
		1	2	3
SS	Present	115.24 N	219.5 N	305.4 N
	ANSYS	116.3 N	225.5 N	312.7 N
CS	Present	196.33 N	282.8 N	439.53 N
	ANSYS	194.7 N	287.6 N	444.51 N

Table 4.13 Dimensional buckling load of symmetric angle–ply (60/-60/-60/60) square thin laminates with different boundary conditions (a/h=20) (material 3)

Boundary Conditions	Method	Mode Serial Number		
		1	2	3
SS	Present	109.39 N	193.213 N	322.19 N
	ANSYS	109.6 N	191.13 N	325.37 N
CS	Present	161.4 N	279.1 N	370.5 N
	ANSYS	160.6 N	280.4 N	377.7 N

Table 4.14 Dimensional buckling load of symmetric cross–ply (0/ 90/ 90/ 0) square thin laminates with different boundary conditions (a/h=20) (material 3)

Boundary Conditions	Method	Mode Serial Number		
		1	2	3
SS	Present	93.4 N	170.4 N	329 N
	ANSYS	94.4 N	181.4 N	315 N
CS	Present	244.5 N	263.7 N	366.23 N
	ANSYS	244.4 N	265.8 N	369.6 N

4.2.3 Comparisons with Experimental Results

Many numerical and mathematical models exist which can be used to describe the behavior of a laminate under the action of different forces. When it comes to buckling, a mathematical model can be developed which is used to model the phenomenon of buckling. But numerical methods become complicated as the number of assumptions and variables increase. Also, once the model is formed, it takes a lot of time to solve the partial differential equations and then arrive to the final result. This process becomes very cumbersome and time consuming. In view of the above-mentioned limitations, experimental methods are followed. The experimental process needs less time and less computational work. Also, the results obtained in experiments are fairly close to that which is obtained theoretically.

The composites have two components. The first is the matrix which acts as the skeleton of the composite and the second is the hardener which acts as the binder for the matrix. The reinforcement that was used for the present study was woven glass fibers. Glass fibers are materials which consist of numerous extremely fine fibers of glass. The hardener that utilized was epoxy which functions as a solid cement to keep fiber layers together.

To manufacture the composites the following steps were taken:
1. The weight of the fiber was noted down, then approximately 1/3rd mass of epoxy was prepared for further use.
2. A clean plastic sheet was taken and the mold releasing spray was sprayed on it. After that, a generous coating of the hardener mixture was coated on the sheet. A woven fiber sheet was taken and placed on top of the coating. A second coating was done again, and a second layer of fiber was placed, and the process continued until the required thickness was obtained. The fiber was pressed with the help of rollers.
3. Another plastic sheet was taken and the mold releasing spray was sprayed on it. The plastic sheet was placed on top of the fiber with hardener coating.
4. The plate obtained was placed under weights for a period of 24 hours.
5. After that the plastic sheets were removed and the plates separated.

The buckling test rig for biaxial compression was developed in Tehran University of Science and Technology, College of Engineering, Iran. The frame was built using rectangular shaped mild steel channels. The channels were welded to one another and then the frame was prepared. A two-ton hydraulic jacks were assembled into the frame to provide the necessary hydraulic forces for biaxial compression of the plates. The setup can be easily assembled and disassembled. Thus, the setup offers flexibility over the traditional buckling setups.

It is proposed to undertake some study cases and obtain experimental results of non – dimensional buckling of rectangular laminated plates subjected to in – plane biaxial Compressive loads. The plates are assumed to be either simply supported on all edges (SS), or a combined case of clamped and simply supported (CS), or clamped on all edges (CC).

The effects of various parameters like material anisotropy, fiber orientation, aspect ratio, and edge conditions on the buckling load of laminated plates are to be investigated and compared with the present finite element results. The plates are made of graphite – epoxy material (material 3), and generally square with side $a = b = 250mm$ and length to thickness ratio (a/h)=20. The required experiments are explained below:

Experiment (1): Effect of Material Anisotropy (E_1/E_2)

Cross – ply symmetric laminates with length to thickness ratio of ($a/h = 20$) are to be tested. The ratio of longitudinal to transverse modulus (E_1/E_2) is to be increased from 10 to 50. The required number of plies is 8. The plate is simply – supported (SS) on all edges. The experimental values of buckling load were compared with the present theoretical results as shown in table 4.15.

Table 4.15 Effect of material anisotropy on buckling load $a/h = 20$

E_1/E_2	Method	Buckling loads
10	Present	0.5537
	Experimental	0.4985
20	Present	0.4789
	Experimental	0.4310
30	Present	0.4536
	Experimental	0.4082
40	Present	0.4418
	Experimental	0.3976
50	Present	0.4343
	Experimental	0.3908

It is observed that the buckling load decreases with the increase in material anisotropy (E_1/E_2). The present theoretical results were about 10% higher than the experimental values which is considered to be acceptable.

Experiment (2): Effect of Fiber Orientation (θ)

Symmetric and anti – symmetric cross – ply laminated plates (0/ 90/ 90/ 0) and (0/ 90/ 0/ 90) with length to thickness ratio (a/h) are to be tested. The required number of plies is 8. The plate is simply supported (SS) on four edges. As shown in table 4.16 below, the theoretical buckling load was found to be 10% above the experimental value.

Table 4.16 Effect of fiber orientation on buckling load $E_1/E_2 = 40$, $a/h = 20$

Orientation	Method	Buckling loads
Symmetric	Present	0.4418
	Experimental	0.3976
Anti – Symmetric	Present	0.4417
	Experimental	0.3975

Experiment (3): Effect of Aspect Ratio (a/b)

The effect of aspect ratio (a/b) on the buckling load is studied by testing cross – ply symmetric (0/ 90/ 90/ 0) laminates with length to thickness ratio $(a/h = 20)$. The aspect ratios 0.5, 1, 1.5 and 2.0 are to be tested. The required number of plies is 8. The plate is simply supported on four edges and the modulus ratio is taken to be $(E_1/E_2 = 40)$. As shown in table 4.17 below, the difference between the theoretical and experimental buckling was found to be about 10%.

Table 4.17 Effect of aspect ratio on buckling load $E_1/E_2 = 40$, $a/h = 20$

Aspect Ratio (a/b)	Method	Buckling loads
0.5	Present	0.4192
	Experimental	0.3773
1.0	Present	0.4418
	Experimental	0.3976
1.5	Present	0.7187
	Experimental	0.6468
2.0	Present	1.2324
	Experimental	1.1092

Experiment (4): Effect of Boundary Conditions

Cross – ply symmetric laminates (0/ 90/ 90/ 0) can be used to study the effect of the boundary conditions on the buckling load. The length to thickness ratio is taken to be $(a/h = 20)$. The boundary conditions used are SS, CS and CC. The required number of plies is 8 and the modulus ratio (E_1/E_2) is selected to be 40. As shown in table 4.18 below, the same difference between the theoretical and experimental results was observed.

Table 4.18 Effect of boundary conditions on buckling load $E_1/E_2 = 40$, $a/h = 20$

Boundary Conditions	Method	Buckling loads
SS	Present	0.4418
	Experimental	0.3976
CS	Present	1.2882
	Experimental	1.1594
CC	Present	1.3812
	Experimental	1.2431

6. CONCLUSIONS

A Fortran program based on finite elements (FE) has been developed for buckling analysis of thin rectangular laminated plates using classical laminated plate theory (CLPT). The problem of buckling loads of generally layered composite plates has been studied. The problem is analyzed and solved using the energy approach, which is formulated by a finite element model. In this method, quadrilateral elements are applied utilizing a four noded model. Each element has three degrees of freedom at each node. The degrees of freedom are: lateral displacement (w), and rotation (ϕ) and (ψ) about the x and y axes respectively. To verify the accuracy of the present technique, buckling loads are evaluated and validated with other works available in the literature. Further

comparisons were carried out and compared with the results obtained by the ANSYS package and the experimental result. The good agreement with available data demonstrates the reliability of finite element method used.

ACKNOWLEDGEMENT

The author would like to acknowledge with deep thanks and profound gratitude Mr. Osama Mahmoud Mohammed Ali of Daniya Center for Publishing and Printing Services, Atbara, who spent many hours in editing, re – editing of the manuscript in compliance with the standard format of International Journal of Engineering Research and Advanced Technology (IJERAT).

REFERENCES

[1] Reissner E. and Stavsky Y.,' Bending and stretching of certain types of heterogeneous Aeolotropic plates', Journal of applied mechanics, vol.28; (1961): PP. (402– 408).

[2] Srinivas S. and Rao A.K.,' Bending, vibration and buckling of simply supported thick orthotropic rectangular plates and laminates', vol.6; (1970): PP. (1463 –1481).

[3] L. H. Yu, and C. Y. Wang, 'Buckling of rectangular plates on an elastic foundation using the levy solution', American Institute of Aeronautics and Astronautics, 46; (2008): PP. (3136 – 3167).

[4] M. Mohammadi, A. R. Saidi, and E. Jomehzadeh, 'Levy solution for buckling analysis of functionally graded rectangular plates', International Journal of Applied Composite Materials, 10; (2009): PP. (81 – 93).

[5] Moktar Bouazza, Djamel Ouinas, Abdelaziz Yazid and Abdelmadjid Hamouine, 'Buckling of thin plates under uniaxial and biaxial compression', Journal of Material Science and Engineering B2, 8; (2012): PP. (487 – 492).

[6] Mahmoud Yassin Osman and Osama Mohammed Elmardi Suleiman, 'Buckling analysis of thin laminated composite plates using finite element method', International Journal of Engineering Research and Advanced Technology (I JERAT), Volume 3, Issue 3; March (2017): PP. (1 – 18).

[7] J. N. Reddy, 'Mechanics of laminated composite plates and shells, theory and analysis', second edition, CRC press, Washington; (2004).

APPENDICES

Appendix (A)

The transformed material properties are:

$$C_{11} = C'_{11}cos^4\theta + C'_{22}sin^4\theta + 2(C'_{12} + 2C'_{66})sin^2\theta cos^2\theta$$
$$C_{12} = (C'_{11} + C'_{22} - 4C'_{66})sin^2\theta cos^2\theta + C^1_{12}(cos^4\theta + sin^4\theta)$$
$$C_{22} = C'_{11}cos^4\theta + C'_{22}sin^4\theta + 2(C'_{12} + 2C'_{66})sin^2\theta cos^2\theta$$
$$C_{16} = (C'_{11} - C'_{12} - 2C'_{66})cos^3\theta sin\theta - (C'_{22} - C'_{12} - 2C'_{66})sin^3\theta cos\theta$$
$$C_{26} = (C'_{11} - C'_{12} - 2C'_{66})cos\theta sin^3\theta - (C'_{22} - C'_{12} - 2C'_{66})sin\theta cos^3\theta$$
$$C_{66} = (C'_{11} - C'_{22} - 2C'_{12} - 2C'_{66})sin^2\theta cos^2\theta + C'_{66}(sin^4\theta + cos^4\theta)$$

where $C'_{11} = \frac{E_1}{1 - \nu_{12}\nu_{21}}$, $C'_{22} = \frac{E_2}{1 - \nu_{12}\nu_{21}}$, $C'_{16} = G_{12}$

Appendix (B)

$a_{i,j}/8$

N_i \ i	$i,1$	$i,2$	$i,3$	$i,4$	$i,5$	$i,6$	$i,7$	$i,8$	$i,9$	$i,10$	$i,11$	$i,12$
N_1	2	-3	3	0	-4	0	1	0	0	-1	1	1
N_2	1	-1	1	-1	-1	0	1	-1	0	0	1	0
N_3	-1	1	-1	0	1	1	0	0	-1	1	0	-1
N_4	2	-3	-3	0	4	0	1	0	0	1	-1	-1
N_5	1	-1	-1	-1	1	0	1	1	0	0	-1	0
N_6	1	-1	-1	0	1	-1	0	0	1	1	0	-1
N_7	2	3	3	0	4	0	-1	0	0	-1	-1	-1
N_8	-1	-1	-1	1	-1	0	1	1	0	0	1	0
N_9	-1	-1	-1	0	-1	1	0	0	1	1	0	1
N_{10}	2	3	-3	0	-4	0	-1	0	0	1	1	1
N_{11}	-1	-1	1	1	1	0	1	-1	0	0	-1	0
N_{12}	1	1	-1	0	-1	-1	0	0	-1	1	0	1

Appendix (C)

The integrals in equations (13) and (14) are given in nondimensional form as follows:

$$\iint \frac{\partial^2 N_i}{\partial x^2}\frac{\partial^2 N_j}{\partial x^2}\,dx\,dy = \frac{4k}{h^3}\iint \frac{\partial^2 N_i}{\partial r^2}\frac{\partial^2 N_j}{\partial r^2}\,dr\,ds$$

$$= \frac{4n^3}{mR}\left(16a_{i,4}\,a_{j,4} + 48a_{i,7}a_{j,7} + 16a_{i,8}a_{j,8}/3 + 16a_{i,11}a_{j,11}\right)$$

$$\iint \frac{\partial^2 N_i}{\partial y^2}\frac{\partial^2 N_j}{\partial y^2}\,dx\,dy = \frac{4h}{k^3}\iint \frac{\partial^2 N_i}{\partial s^2}\frac{\partial^2 N_j}{\partial s^2}\,dr\,ds$$

$$= \frac{4m^3R^3}{n}\left(16a_{i,6}\,a_{j,6} + 16a_{i,9}a_{j,9}/3 + 48a_{i,10}a_{j,10} + 16a_{i,12}a_{j,12}\right)$$

$$\iint \frac{\partial^2 N_i}{\partial x^2}\frac{\partial^2 N_j}{\partial y^2}\,dx\,dy = \frac{4}{kh}\iint \frac{\partial^2 N_i}{\partial r^2}\frac{\partial^2 N_j}{\partial s^2}\,dr\,ds$$

$$= 4mnR\left(16a_{i,4}\,a_{j,6} + 16a_{i,7}a_{j,9} + 16a_{i,8}a_{j,10} + 16a_{i,11}a_{j,12}\right)$$

$$\iint \frac{\partial^2 N_i}{\partial y^2}\frac{\partial^2 N_j}{\partial x^2}\,dx\,dy = \frac{4}{kh}\iint \frac{\partial^2 N_i}{\partial s^2}\frac{\partial^2 N_j}{\partial r^2}\,dr\,ds$$

$$= 4mnR\left(16a_{i,6}\,a_{j,4} + 16a_{i,9}a_{j,7} + 16a_{i,10}a_{j,8} + 16a_{i,12}a_{j,11}\right)$$

$$\iint \frac{\partial^2 N_i}{\partial x\partial y}\frac{\partial^2 N_j}{\partial x\partial y}\,dx\,dy = \frac{4}{kh}\iint \frac{\partial^2 N_i}{\partial r\partial s}\frac{\partial^2 N_j}{\partial r\partial s}\,dr\,ds$$

$$= 4mnR\left[4a_{i,5}\,a_{j,5} + 4(3a_{i,5}a_{j,11} + 4(a_{i,8}a_{j,8})/3\right.$$

$$+4(3a_{i,5}\,a_{j,12} + 4a_{i,9}a_{j,9})/3 + 4(a_{i,11}\,a_{j,12} + a_{i,12}a_{j,11})$$

$$\left.+ 36a_{i,12}a_{j,12}/5\right]$$

$$\iint \frac{\partial N_i}{\partial x}\frac{\partial N_j}{\partial x}\,dx\,dy = \frac{k}{h}\iint \frac{\partial N_i}{\partial r}\frac{\partial N_j}{\partial r}\,dr\,ds$$

$$= \frac{n}{mR}\left[4a_{i,2}\,a_{j,2} + 4(3a_{i,2}a_{j,7} + 4a_{i,4}a_{j,4} + 3a_{i,7}a_{j,2})/3\right.$$

$$+4(a_{i,2}a_{j,9} + a_{i,5}a_{j,5} + a_{i,9}a_{j,2})/3 + 4(3a_{i,5}\,a_{j,11} + 3a_{i,7}a_{j,9} + 4a_{i,8}a_{j,8}$$

$$+3a_{i,9}a_{j,7} + 3a_{i,11}a_{j,5})/9 + 4(a_{i,5}a_{j,12} + a_{i,9}a_{j,9} + a_{i,12}a_{j,5})/5$$

$$\left.+36a_{i,7}a_{j,7}/5 + 12a_{i,11}a_{j,11}/5 + 4(a_{i,11}a_{j,12} + a_{i,12}a_{j,11})/5 + 4a_{i,12}a_{j,12}/7\right]$$

$$\iint \frac{\partial N_i}{\partial y}\frac{\partial N_j}{\partial y}\,dx\,dy = \frac{h}{k}\iint \frac{\partial N_i}{\partial s}\frac{\partial N_j}{\partial s}\,dr\,ds$$

$$= \frac{mR}{n}\left[4a_{i,3}\,a_{j,3} + 4(a_{i,3}a_{j,8} + a_{i,5}a_{j,5} + a_{i,8}a_{j,3})/3\right.$$

$$+4(3a_{i,3}a_{j,10} + 4a_{i,6}a_{j,6} + 3a_{i,10}a_{j,3})/3 + 4(3a_{i,5}\,a_{j,11} + a_{i,8}a_{j,8} + a_{i,11}a_{j,5})/5$$

$$+4(3a_{i,5}a_{j,12} + 3a_{i,8}a_{j,10} + 4a_{i,9}a_{j,9} + 3a_{i,10}a_{j,8} + 3a_{i,12}a_{j,5})/9$$

$$\left.+36a_{i,10}a_{j,10}/5 + 4(a_{i,11}a_{j,12} + a_{i,12}a_{j,11})/5 + 12a_{i,12}a_{j,12}/5 + 4a_{i,11}a_{j,11}/7\right]$$

$$\iint \frac{\partial N_i}{\partial x}\frac{\partial N_j}{\partial y}\,dx\,dy = \iint \frac{\partial N_i}{\partial r}\frac{\partial N_j}{\partial s}\,dr\,ds$$
$$= 4a_{i,2}a_{j,3} + 4(a_{i,2}a_{j,8} + 2a_{i,4}a_{j,5} + 3a_{i,7}\,a_{j,8})/3 + 4(3\,a_{i,2}a_{j,10} + 2a_{i,5}a_{j,6}$$
$$+3a_{i,9}a_{j,3})/3 + 4(2a_{i,4}a_{j,11} + 3a_{i,7}a_{j,8})/5 + 4(6a_{i,4}a_{j,12} + 9a_{i,7}a_{j,10} + 4a_{i,8}a_{j,9}$$
$$+a_{i,9}a_{j,8} + 6a_{i,11}a_{j,6})/9 + 4(3a_{i,9}a_{j,10} + 2a_{i,12}a_{j,6})/5$$
$$\iint \frac{\partial N_i}{\partial y}\frac{\partial N_j}{\partial x}\,dx\,dy = \iint \frac{\partial N_i}{\partial s}\frac{\partial N_j}{\partial r}\,dr\,ds$$
$$= 4a_{i,3}a_{j,2} + 4(3a_{i,3}a_{j,7} + 2a_{i,5}a_{j,4} + a_{i,8}\,a_{j,2})/3 + 4(3\,a_{i,3}a_{j,9} + 2a_{i,6}a_{j,5}$$
$$+3a_{i,10}a_{j,2})/3 + 4(6a_{i,6}a_{j,11} + a_{i,8}a_{j,9} + 4a_{i,9}a_{j,8} + 9a_{i,10}a_{j,7} + 6a_{i,2}a_{j,4})/9$$
$$+4(2a_{i,6}a_{j,12} + 3a_{i,10}a_{j,9})/5 + 4(3a_{i,8}a_{j,7} + 2a_{i,11}a_{j,4})/5$$
$$\iint \frac{\partial^2 N_i}{\partial x^2}\frac{\partial^2 N_j}{\partial x\partial y}\,dx\,dy = \frac{4}{h^2}\iint \frac{\partial^2 N_i}{\partial r^2}\frac{\partial^2 N_j}{\partial r\partial s}\,dr\,ds$$
$$= 4n^2\left[8a_{i,4}\left(a_{j,5} + a_{j,11} + a_{j,12}\right) + 16(2a_{i,7}a_{j,8} + a_{i,8}a_{j,9}/3)\right]$$
$$\iint \frac{\partial^2 N_i}{\partial x\partial y}\frac{\partial^2 N_j}{\partial x^2}\,dx\,dy = \frac{4}{h^2}\iint \frac{\partial^2 N_i}{\partial r\partial s}\frac{\partial^2 N_j}{\partial r^2}\,dr\,ds$$
$$= 4n^2\left[8a_{i,4}\left(a_{i,5} + a_{i,11} + a_{i,12}\right) + 16a_{i,8}a_{j,7} + 16a_{i,9}a_{j,8}/3\right]$$
$$\iint \frac{\partial^2 N_i}{\partial y^2}\frac{\partial^2 N_j}{\partial x\partial y}\,dx\,dy = \frac{4}{k^2}\iint \frac{\partial^2 N_i}{\partial s^2}\frac{\partial^2 N_j}{\partial r\partial s}\,dr\,ds$$
$$= 4m^2R^2\left[8a_{i,6}\left(a_{j,5} + a_{j,11} + a_{j,12}\right) + 16a_{i,10}a_{j,9} + 16a_{i,9}a_{j,8}/3\right]$$
$$\iint \frac{\partial^2 N_i}{\partial x\partial y}\frac{\partial^2 N_j}{\partial y^2}\,dx\,dy = \frac{4}{k^2}\iint \frac{\partial^2 N_i}{\partial r\partial s}\frac{\partial^2 N_j}{\partial s^2}\,dr\,ds$$
$$= 4m^2R^2\left[8a_{i,6}\left(a_{i,5} + a_{i,11} + a_{i,12}\right) + 16a_{i,9}a_{j,10} + 16a_{i,8}a_{j,9}/3\right]$$

In the above expressions $h = \frac{a}{n},\ k = \frac{b}{m}$ where a and b are the dimensions of the plate in the x – and y – directions respectively. n and m are the number of elements in the x – and y – directions respectively. Note that $dx = \frac{h}{2}dr$ and $dy = \frac{k}{2}ds$ where r and s are the normalized coordinates, and $R = a/b$.